Energy Considerations for WiFi Offloading of Video Streaming

Valentin Burger[1], Fabian Kaup[2], Michael Seufert[1], Matthias Wichtlhuber[2], David Hausheer[2], Phuoc Tran-Gia[1]

[1] University of Würzburg, Insitute of Computer Science, Würzburg, Germany, {burger | seufert | trangia}@informatik.uni-wuerzburg.de
[2] TU Darmstadt, Peer-to-Peer Systems Engineering Lab, Darmstadt, Germany, {fabian.kaup | mwichtlh | hausheer}@ps.tu-darmstadt.de

Abstract. The load on cellular networks is constantly increasing. Especially video streaming applications, whose demands and requirements keep growing, put high loads on cellular networks. A solution to mitigate the cellular load in urban environments is offloading mobile connections to WiFi access points, which is followed by many providers recently. Because of the large number of mobile users and devices there is also a high potential to save energy by WiFi offloading. In this work, we develop a model to assess the energy consumption of mobile devices during video sessions. We evaluate the potential of WiFi offloading in an urban environment and the implications of offloading connections on energy consumption of mobile devices. Our results show that, although WiFi is more energy efficient than 3G and 4G for equal data rates, the energy consumption increases with the amount of connections offloaded to WiFi, due to poor data rates obtained for WiFi in the streets. This suggests further deployment of WiFi access points or WiFi sharing incentives to increase data rates for WiFi and energy efficiency of mobile access.

Key words: WiFi Offloading, Energy Efficiency, Cellular Networks, Mobile Access, Video on Demand, Modelling, Performance Evaluation

1 Introduction

Cellular networks are facing an ever-increasing growth of data traffic combined with immense demands for service and quality. Especially video streaming, being a popular, data-intensive, and quality-sensitive service, contributes to this load as it accounts for 55% (1.38 exabytes) of all mobile traffic by the end of 2014. As the number of mobile devices is increasing, also mobile traffic is expected to grow. The demanding video streaming will reinforce its position and its share is expected to rise up to 72% (17.45 exabytes) in 2019. [8]

A new trend to handle these huge demands of mobile users and to reduce the load on cellular networks is WiFi offloading [29]. Thereby, users connect to WiFi access points instead of cellular base stations. Thus, the traffic flows through well-dimensioned fixed networks, which is more efficient for providers both in terms of cost and energy. In addition, end users can benefit from higher throughput and

avoid exceeding their data plan. Due to the growing WiFi infrastructure (e.g., in cities like Berlin [3], London [1], or Singapore [4]) and independently operated free public WiFi hotspots (e.g, provided by cafes, shops, libraries), which can be found in hotspot databases like WeFi[1], offloading is increasingly available. In 2014, already 45% of the total mobile data was offloaded onto the fixed network through WiFi or small-cells, and this ratio is expected to increase up to 54% in 2019 [8].

In this work, we investigate the energy efficiency of WiFi offloading for video streaming, which is among the most popular and demanding Internet services. We present a framework for the simulative evaluation of video streaming energy consumption for mobile users. The simulation framework is based on citywide connectivity measurements and uses a simple streaming model, which allows for an assessment of the resulting data transmission bursts. We evaluate the energy consumption of these bursts for WiFi offloading based on different WiFi sharing percentages, i.e., percentage of accessible WiFi hotspots, and different cellular technologies. Thus, we are able to assess in which cases the energy consumption of video streaming can be improved by WiFi offloading or not.

Our results show that for equal data rates WiFi connections consume less energy, than cellular connections. Independent of the access technology the energy consumption decreases exponentially with the data rate. As the data rates for WiFi measured in the streets of an urban city center are rather low compared to 3G and 4G, offloading connections for video sessions to WiFi increases the energy consumption of mobile devices. However, minimal energy consumption is obtained for WiFi connections with high throughput. This suggests deploying WiFi access points or providing incentives for WiFi sharing to obtain high data rates while reducing energy consumption of mobile devices.

The paper is structured as follows. Background and research on WiFi offloading and mobile video streaming are outlined in Section 2. Section 3 presents the measurement setup, the resulting data set, and the simulation framework. The results, which were obtained through the simulation framework, are described in Section 4 and Section 5 concludes.

2 Background and Related Work

WiFi offloading has been widely adopted in commercial services and is also in the focus of research works. Ubiquitous Internet access via WiFi is offered by specialized WiFi-sharing communities (e.g., Fon[2]) but also by big telecommunication operators (e.g., BT[3]) to provide their users fast access bandwidth and reduce the load on mobile networks. Incentives and algorithms for Internet access sharing are investigated in [18] and many works focus on the deployment of architectures for ubiquitous WiFi access in metropolitan areas [24, 28, 9]. Systems

[1] http://wefi.com/
[2] http://www.fon.com
[3] http://www.btwifi.co.uk/

for sharing WiFi passwords via online social network apps with trusted friends are described in [17, 10, 25]. Offloading in heterogeneous networks is modeled and analyzed in [26]. [16] presents available features for mobile traffic offloading, and [12, 19, 7] show that multipath TCP can be utilized for handovers between WiFi and mobile networks. [11] outlines approaches, which enable mobility and multihoming. Finally, WiFi onloading [23] is an opposed concept, which utilizes different peaks in mobile and fixed networks to onload data to the mobile network to support applications on short time scales.

The mobile network quality (WiFi/cellular) must be known to determine the energy consumption of individual connections. A number of studies focuses on analyzing the mobile network performance in terms of RTT and throughput of the user [30, 27, 22]. The expected performance for different network technologies can be derived from these data.

Energy models for smartphones were derived in a number of publications [5, 31, 13] for different devices and network technologies. Still, due to the steady progress in hardware development and changes in the network infrastructure and configuration, the transferability of these models is limited. Balasubramanian et al. [5] analyzed the influence of different network interfaces on the energy cost of different data transmissions. Power models for WiFi, 2G, and 3G connections including the connection setup and tear-down cost are analyzed, with the goal of developing an algorithm reducing the energy wasted in ramp and tail states. Zhang et al. [31] describe an approach to reduce the effort for creating power models for smartphones. This is demonstrated on the HTC One (hardware similar to the Nexus One), from which a detailed power model including the 3G power states is derived. Huang et al. [13] present a detailed analysis of the power characteristics of 4G networks in the US. Using the data from a dedicated user study, the different network states, their duration and power consumption are derived. From these models the energy cost of loading different web-pages is derived.

Comparative measurements conducted on the Nexus 5 still show a different picture. The ramp and tail states measured in 2014 are considerably shorter compared to [13]. Also, the measured data rates are considerably higher. Hence, in this work the results of independent measurements are used that were conducted on the Nexus 5, resulting in realistic power models for an operational 4G network in 2014.

3 Measurement and Model

In order to derive locations of mobile users in an urban area and the location and throughput of WiFi access points, we use different data sets and models. In the following the data sets derived by mobile network measurements and existing data sets are described. Further on, the video on demand traffic model and the applied energy model for mobile devices is described.

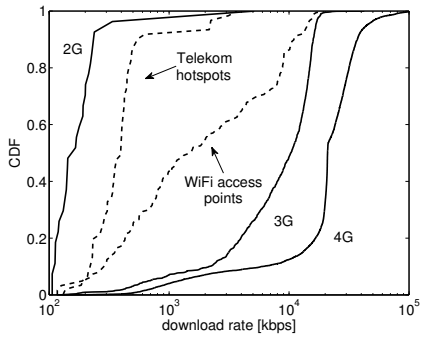

Fig. 1: Throughput of mobile connections for different access technologies.

3.1 Data Sets

To derive the throughput of mobile connections, we use the network performance data set, as described in [6]. The data was gathered in and around Darmstadt, Germany, using the NetworkCoverage App[4] [14]. For details please refer to [6, 14]. The measurement consist of 4436 4G connections, 1043 3G, 23 2G, and 173 WiFi connections. The WiFi measurements were conducted mainly outdoors and reflect the variability of WiFi access rates.

Figure 1 shows the cumulative distribution function of the down-link throughput for different mobile access technologies. WiFi access is distinguished between hotspots by a major German provider (i.e., Deutsche Telekom) and other WiFi access points. Less than 10% of connections with Telekom hotspots achieve a throughput higher than 10^3kbps. Since we investigate the potential of shared WiFi access points, we only consider the throughput of the other WiFi access points, which have a throughput higher than 10^3kbps in 60% of the cases. 3G and 4G connections have highest throughput, where about half of the 3G connections get more than 10^4kbps and almost 90% of the 4G connections.

To derive the location of WiFi access points in Darmstadt, a data set is used, consisting of 1527 AP locations measured in the inner city of Darmstadt. The measured APs are a mix of open and private APs, and hence are expected to match common usage patterns. In [20] the locations of the access points were interpolated from the observed WiFi beacons at street level.

In order to determine the location of end-users in the Darmstadt city area a street map of Darmstadt from OpenStreetMap [2] is used. As locations for end-users we use the way points provided in the street map that describe buildings, facilities, local businesses or sights. The way points are interconnected and used to define streets. The way points are all set up by users contributing to the OpenStreetMap platform.

[4] `https://play.google.com/store/apps/details?id=de.tudarmstadt.networkcoverage` accessed: 2015-01-21

3.2 Video on Demand Traffic Model

To evaluate the energy efficiency of mobile video requests the traffic bursts generated in a video session have to be analyzed. For that purpose the arrivals and volumes of the traffic bursts need to be known. Current video streaming platforms and clients use an algorithm based on thresholds of the playback buffer to stream the video data with HTTP Range requests. This algorithm tries to maintain a certain level of the playback buffer that ensures smooth video playback and prevents the video from stalling, while keeping the amount of downloaded video data low.

To derive the bit rate and duration of videos streamed by mobile devices we use the results from [21] where the video formats in mobile networks were characterized by analysing 2000 videos streamed from the video on demand platform YouTube. The format selected depends on the YouTube player of the terminal used. The authors find that terminals using Android and iOS select format *itag*36 in more than 80% of the streams. Figure 2 shows the cumulative distribution of video bit rates of the codec and durations for mobile videos in *itag*36. The majority of the videos have a bit rate between 220 and 250 kbps.

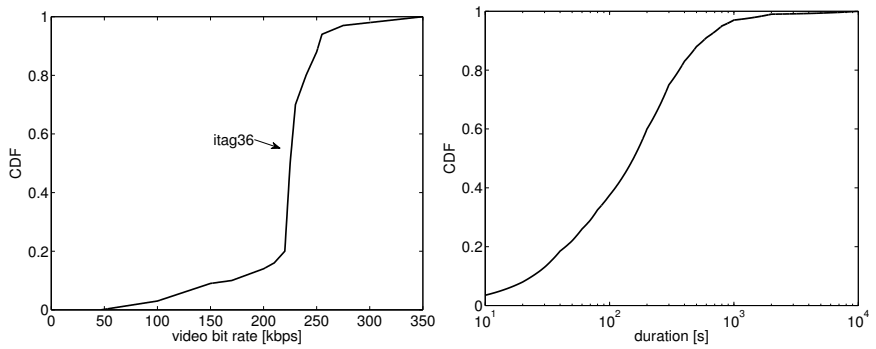

(a) Bit rate (b) Duration

Fig. 2: Bit rate and duration of YouTube videos in *itag*36 format [21].

We generate video requests by a Poisson process with rate λ. For each video request i we determine the duration d_i and mean bit rate b_i according to the empiric cumulative distributions from [21]. The volume of the video equals $v_i = d_i \cdot b_i$. We define two thresholds α and β in unit of seconds for the playback time buffered. If the buffered playback time drops below threshold α video data is downloaded and the buffer is filled. If the playback time buffered exceeds β the download of video data is paused and the traffic burst ends. At the time video i is requested $t_i = t_{i_1}$, the first traffic burst i_1 is downloaded. The video playback starts after the playback time buffered exceeds threshold α the first time. The throughput ρ_{i_j} received for burst j of request i is determined randomly according

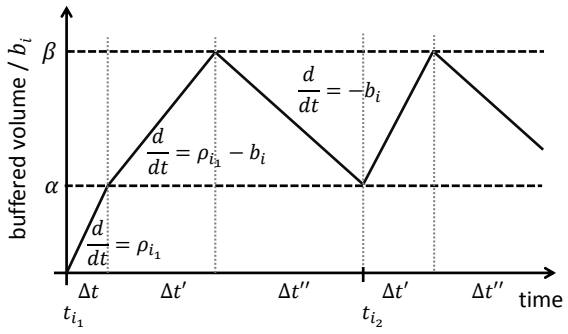

Fig. 3: Playback buffer in case of $\rho_{i_j} > b_i$.

to the access technology and its cumulative distribution function derived from the network performance data set described in Sec. 3.1. The time a traffic burst i_{j+1} is downloaded depends on the throughput ρ_{i_j} received for the preceding traffic burst i_j.

1. Case $\rho_{i_j} \leq b_i$:
   If $\rho_{i_j} \leq b_i$ the throughput is not high enough to increase the playback buffer. That means threshold β will not be reached, and the rest of the video data will be downloaded within burst i_j omitting burst i_{j+1}. In this case, the volume of burst i_j equals the volume of the remaining video data:

$$v_{i_j} = \begin{cases} v_i & j = 1, \\ v_i - \sum_{k=1}^{j-1} v_{i_k} & j > 1. \end{cases} \tag{1}$$

   This also covers the case where the buffer runs dry and the video stalls, requiring a new pre-buffering phase for alpha seconds buffered video.
2. Case $\rho_{i_j} > b_i$:
   If $\rho_{i_j} > b_i$ the burst download can be divided in 3 phases with durations Δt, $\Delta t'$ and $\Delta t''$, c.f., figure 3.
   In the first phase, the video is pre-buffered, while the playback of the video is not yet started. This phase only exists for the first burst. Video data is downloaded with rate $\frac{d}{dt} = \rho_{i_j}$ until the threshold α is reached, i.e., $\alpha \cdot b_i = \rho_{i_j} \cdot \Delta t$ and

$$\Delta t = \frac{\alpha \cdot b_i}{\rho_{i_j}}. \tag{2}$$

   In the second phase, the playback buffer is filled until it reaches β while the video plays with bit rate b_i. Hence, the gradient of the buffer volume is $\frac{d}{dt} = \rho_{i_j} - b_i$ and video data with bit rate b_i is downloaded, containing $\beta - \alpha$ playback buffer. That means $(\beta - \alpha) \cdot b_i = (\rho_{i_j} - b_i) \cdot \Delta t'$ and

$$\Delta t' = \frac{(\beta - \alpha) \cdot b_i}{\rho_{i_j} - b_i}. \tag{3}$$

In the third phase, the traffic burst ends and the download of video data is paused until the buffer drops below α. During playback the buffer decreases with gradient $\frac{d}{dt} = -b_i$, hence $(\alpha - \beta) \cdot b_i = -b_i \cdot \Delta t''$ and

$$\Delta t'' = \frac{(\alpha - \beta) \cdot b_i}{-b_i} = \beta - \alpha. \tag{4}$$

The time of burst i_{j+1} is calculated by adding the duration of the phases Δt, $\Delta t'$ and $\Delta t''$:

$$t_{i_{j+1}} = \begin{cases} t_{i_j} + \frac{\alpha \cdot b_i}{\rho_{i_j}} + \frac{(\beta-\alpha) \cdot b_i}{\rho_{i_j} - b_i} + (\beta - \alpha) & j = 1, \\ t_{i_j} + \frac{(\beta-\alpha) \cdot b_i}{\rho_{i_j} - b_i} + (\beta - \alpha) & j > 1. \end{cases} \tag{5}$$

The volume of burst i_j is calculated by accumulating the throughput during Δt and $\Delta t'$:

$$v_{i_j} = \begin{cases} \min(\alpha \cdot b_i + \rho_{i_j} \frac{(\beta-\alpha) \cdot b_i}{\rho_{i_j} - b_i}, v_i) & j = 1, \\ \min(\rho_{i_j} \frac{(\beta-\alpha) \cdot b_i}{\rho_{i_j} - b_i}, v_i - \sum_{k=1}^{j-1} v_{i_k}) & j > 1. \end{cases} \tag{6}$$

Given the arrival times t_{i_j} and volumes v_{i_j} of each burst i_j for video request i, we can calculate the energy consumption of the video requests based on the energy model.

3.3 Energy Model

In this work we focus on the energy consumption of mobile devices, which is most relevant for end-users, rather than also considering the energy consumed in base stations and access points. Due to the vast amount of mobile devices in use, small energy savings per mobile devices sum up to huge energy savings in total. As in [15] the energy consumption for the individual connections is determined by calculating the consumed energy based on power consumption models for the Nexus 5. The measurements were conducted in an office environment with good network availability and signal strength. The measured power consumption is expected to be similar for outdoor and indoor communication, as for commonly used power amplifiers in mobile phones the power consumption does not depend on the output power. For each technology, traffic flows with different data rates were received on the mobile phone while measuring the power consumption of the device using the built in voltage and current sensors. The power consumption of the interface is calculated by keeping the device configuration stable (e.g. display brightness, active components), and later removing the influence of the idle state by subtracting the average power consumption of this state. Such, the power consumption of the individual connections can be derived. The data rates

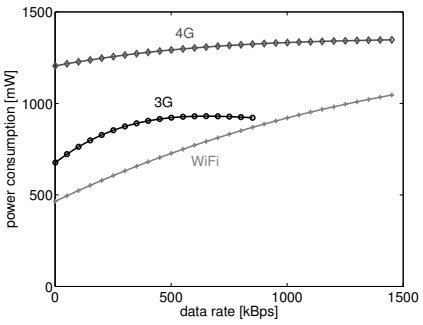

Fig. 4: Power consumption of the interfaces of the Google Nexus 5 at different data rates.

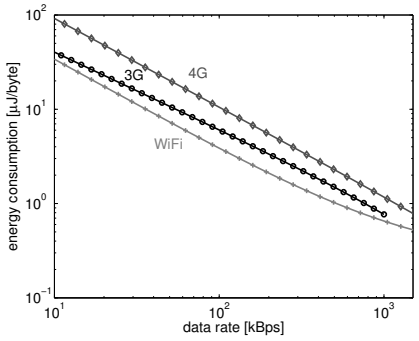

Fig. 5: Energy cost for receiving data on the respective interface of the Google Nexus 5 (excl. cost for ramp and tail).

were adjusted using the linux tool tc with a hierarchical token bucket (HTB) on the server. Hence, no bursty traffic was used for calibration.

The power models as derived from the measurements of Google's Nexus 5 are given in Figure 4. The plot shows the lowest cost for WiFi connections, followed by the 3G and 4G connection. The derived model is valid for the typical data rates achieved on the respective interface.

Figure 4 includes the idle power consumption of the network interface, but not the idle power consumption of the mobile phone. The different offsets and slopes are caused by the different hardware components on the mobile phone. The average energy consumption per byte for a transfer of traffic with size S during time interval T is calculated by $\overline{E} = T \cdot \overline{P(r(t))}/S$, with power P at configured rate $r(t)$. This may be approximated by $E = P(r(t))/r(t)$ for constant bit rates, as in Figure 5, which depicts the power while the interface is active converted to cost per byte transmitted.

The plot shows an exponential decrease of the energy expense per byte transmitted with increasing data rates. This depends on the fact that the idle time of the interface, which has little energy expense, increases with the data rate. The fraction of energy required to transmit one byte is particularly high for low data rates, as for high data rates the constant part is shared between a large number of packets. Analogue to Figure 4, the cost per byte is lowest for WiFi, followed by 3G and 4G. Similar to the power consumption plot, the data rates for 3G approach 900 kBps. Higher data rates are only possible using WiFi or 4G.

The power model used in this publication includes the cost of connecting and disconnecting from the network. This is commonly referred to as ramp and tail energy. The power consumption and duration of these states was determined by evaluating the periods with higher energy consumption compared to the idle state before and after the data transmission. From this, the average power and duration of ramp and tail states is derived, and added to the total energy con-

sumption. The power consumption of an exemplary connection is given in Figure 6. The first 2 vertical markers indicate the begin and end of the ramp state (connecting to the network), while the second pair of markers indicate the end of the data transfer and end of the data connection, resembling the tail of the cellular connection.

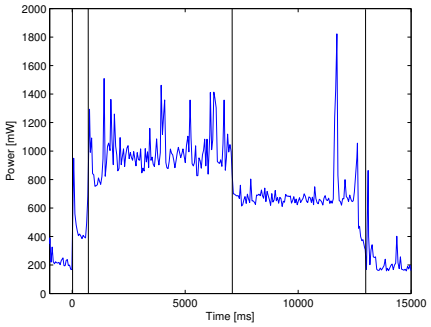

Fig. 6: Exemplary data transfer using the Nexus 5 on 3G. Indicated are the begin and end of the ramp state and begin and end of the tail state

The resulting formula for a continuous data burst i_j with volume v_{i_j} is

$$E_{i_j} = E_{\text{ramp}} + E_{\text{tail}} + \frac{v_{i_j}}{\rho_{i_j}} \cdot P(\rho_{i_j}) = t_{\text{ramp}} \cdot P_{\text{ramp}} + t_{\text{tail}} \cdot P_{\text{tail}} + \frac{v_{i_j}}{\rho_{i_j}} \cdot P(\rho_{i_j}). \quad (7)$$

Further, $P(\rho_{i_j})$ is the interface power consumption during the transmission depending on the data rate ρ_{i_j}. The cost of transmitting at a given data rate is calculated based on the power models of the Nexus 5 as given in Figure 4. For the course of this analysis, the power consumption and the data rate are considered to be constant over the duration of a single burst. The ramp and tail energies were derived from measurements for data transfers of finite duration. The measurements were repeated multiple times leading to the same results. Thus, the ramp and tail energies are considered as constants as given in Table 1.

Table 1: Ramp and tail durations and the derived energy consumption.

	$\mathbf{t}_{\text{ramp}}$ [s]	$\mathbf{t}_{\text{tail}}$ [s]	$\mathbf{E}_{\text{ramp}}$ [J]	$\mathbf{E}_{\text{tail}}$ [J]
3G	1.0	5.0	0.4	3.5
4G	0.1	2.0	0.1	1.2
WiFi	0.2	0.2	0.2	0.1

The individual connections and their duration are identified by iterating through the requested data bursts i_j. If the interval between two bursts i_j and

i_{j+1} is smaller than the ramp and tail durations t_{ramp} and t_{tail}, the bursts are combined and the ramp and tail energies E_{ramp} and E_{tail} are added only once to the energy calculated for request i. This corresponds to the time-out for bearer release in cellular networks.

3.4 Simulation Model

As in [6] we consider an area with a set of way points W and a set of access points A. The location of the way points and access points is specified by longitude and latitude. Each access point $\alpha \in A$ has a fixed transmission range r and is shared with probability p_{share}.

For given transmission range r we define a function $\chi_r : A \times W \mapsto \{0, 1\}$, where χ_r returns 1, only if a way point $w \in W$ is in transmission range of an access point $a \in A$, else 0.

As set of way points W and set of access points A we use the way points from OpenStreetMap in the inner city area of Darmstadt and the interpolated access points described in Sec. 3.1.

The procedure of one run simulating n mobile requests is described in the following. A subset $A_s \subset A$ of shared access points is randomly chosen according to the sharing probability p_{share}. For each mobile request $1 \leq i \leq n$ a random way point $w_i \in W$ is determined. The mobile request i can be offloaded, if a shared WiFi access point is in range, i.e. $\exists a \in A_s | \chi_r(w_i, a) = 1$. With

$$\mathit{off}(i) = \begin{cases} 1, & \exists a \in A_s | \chi_r(w_i, a) = 1\,, \\ 0, & \text{else}\,. \end{cases} \tag{8}$$

the WiFi offloading potential is calculated by the amount of offloaded requests:

$$\overline{\mathit{off}} = \frac{1}{n} \sum_{1 \leq i \leq n} \mathit{off}(i)\,. \tag{9}$$

If the mobile request can be offloaded, WiFi is used as access technology. If the request cannot be offloaded the request is served by the cellular network which uses 3G or 4G access technology, where, according to Sec. 3.1, 4G is available in approximately 4 out of 5 connections, else 3G is used. The throughput ρ_i received for request i is determined randomly according to the access technology and its cumulative distribution function derived from the network performance data set described in Sec. 3.1.

The model is limited in not considering temporal and spatial dynamics of users and cell capacities. The throughput received for a request does not consider the cell load or the load on the WiFi access point and the distance to the antenna. However, the throughput received is derived from real traces, which mitigates these impairments.

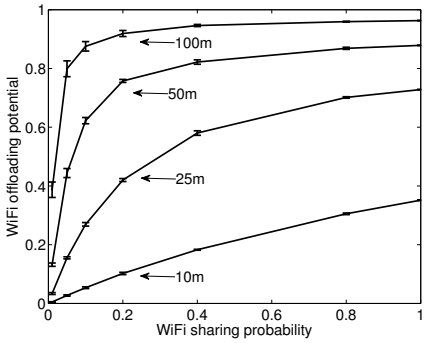

Fig. 7: Amount of mobile connections offloaded to WiFi dependent on sharing probability for different access point transmission ranges.

4 Simulation Results

In the following we describe simulation results to show the WiFi offloading potential in an urban environment dependent on the WiFi sharing probability. The results can be used by operators to assess the feasibility of establishing WiFi offloading according to their cellular network coverage, or to estimate the amount of users that share their access point, which is necessary to get a good WiFi coverage.

The results show mean values with 95% confidence intervals of 10 runs with different random number seeds and $n = 10^6$ mobile requests in each run. We investigate the impact of the WiFi sharing probability on the WiFi offloading potential. As the transmission range of WiFi access points depends on the environment, the number of active connections and its configuration, we show results for different transmission ranges. Figure 7 shows the amount of mobile connections offloaded to WiFi $\overline{off}$ dependent on the WiFi sharing probability p_{share}. The WiFi offloading potential is depicted for different transmission ranges r. If a transmission range of only 10m is assumed, the WiFi offloading potential is rather low and increases almost linearly with the WiFi sharing probability. Roughly every second mobile connection can be offloaded for a transmission range of 25 meters if 40% of the access points are shared and 3 of 4 connections can be offloaded if every access point is shared.

If a WiFi transmission range of 50m is assumed, a decent WiFi offloading potential is obtained if only 10% percent of WiFi access points in an inner city area are shared. Hence, to obtain a good WiFi coverage, incentive mechanisms have to be designed, such that at least 10% of WiFi access points are shared.

We use the traffic model described in Sec. 3.2 together with the energy model described in Sec. 3.3 to evaluate the energy consumption of mobile video requests for different access technologies. The buffer thresholds of the video on demand traffic model are set to $\alpha = 30$s and $\beta = 100$s, according to [21]. To compare

the energy consumption of the mobile access technologies we generate 10^5 video requests for each access technology and calculate the energy consumption. Figure 8 shows the cumulative distribution of the consumed energy in Joule for mobile access technologies 3G, 4G and WiFi. Using 4G as access technology, generally less energy is consumed on the end-device as using 3G. The minimum energy consumption is achieved using WiFi access technology. However, WiFi consumes more energy than 3G in more than 60% of the requests and WiFi consumes more energy than 4G in more than 80% of the requests. This depends on the fact that the energy consumption decreases exponentially with the data rates and that the data rates obtained for WiFi in the measurements are very poor compared to 3G and 4G. Hence, although WiFi is more energy efficient than 3G and 4G for equal data rates, it consumes more energy in this case due to lower data rates.

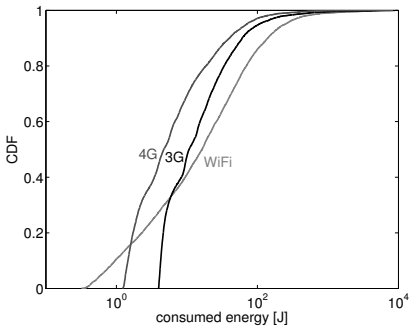

Fig. 8: Energy consumption for different mobile access technologies.

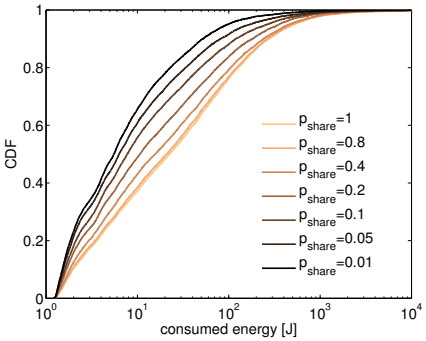

Fig. 9: Energy consumption for different WiFi sharing probabilities.

To investigate the impact of WiFi offloading on the energy consumption of mobile devices, we conduct a parameter study on the sharing probability and set the WiFi transmission range to 25m in the following. We generate 10^5 requests and determine the access technology according to the WiFi offloading simulation described in Sec. 3.4. Figure 9 shows the energy consumption for different WiFi sharing probabilities. The energy consumption generally increases with the WiFi sharing probability. The amount of requests that consume less than 10 Joule decreases about one third if the WiFi sharing probability is increased from 1% to 100%. This depends on the fact that the throughput received for WiFi is rather small in the underlying measurements. For high sharing probabilities there is a saturation effect, because the increase of WiFi coverage diminishes due to the fact that WiFi access points overlap.

Our results show that poor WiFi conditions lead to a higher energy consumption of mobile devices, which offload their video sessions to WiFi. However, the minimum energy consumption for mobile video requests is achieved using WiFi

access technology by receiving a good connection with high throughput. This suggests a high density of WiFi access points to reduce energy consumption of mobile devices and load on cellular networks by WiFi offloading. Here we focus on outdoor users. In the end most video traffic is consumed indoors, where strong WiFi rates and poor cellular rates occur. Considering this, the potential of saving energy by WiFi offloading is even higher according to our results that show low energy consumption for WiFi connections with high throughput.

5 Conclusion

The increasing number of mobile users and the growing popularity of video streaming puts high loads on cellular networks. To cope with this demand, mobile connections can be offloaded to WiFi networks. Especially in urban environments a high coverage of WiFi access points can be beneficial to stream video sessions to mobile devices while keeping their energy consumption low. To investigate the impact of WiFi offloading on the energy consumption of mobile devices during video streaming, we develop a generic model for traffic bursts in current video on demand services and model the energy consumption of current mobile devices for different access technologies. We use existing measurements to derive the throughput of mobile access technologies 3G, 4G, and WiFi in an urban area and develop a simulation model that generates mobile video requests. Applying our models, we assess the energy consumed by mobile video request based on the access technology and received bandwidth. Our results show that slightly increasing WiFi coverage has a high potential to take load off the cellular network. Due to lower throughput compared to 3G and 4G, derived in the provided data sets, the energy consumption increases with the amount of video connections offloaded to WiFi. However, minimal energy consumption is achieved by connections offloaded to WiFi that receive a high throughput. This could be achieved by a high coverage of WiFi access points.

Acknowledgement. This work has been supported in parts by the EU (FP7/#317846, SmartenIT and FP7/#318398, eCOUSIN) and the DFG as part of the CRC 1053 MAKI. The authors would like to acknowledge valuable feedback by the reviewers and comments by their colleagues and project partners.

References

1. City of London WiFi network. URL `https://www.cityoflondon.gov.uk/business/commercial-property/utilities-and-infrastructure-/Pages/wi-fi.aspx`
2. OpenStreetMap. URL `http://www.openstreetmap.org/export#map=14/49.8788/8.6628`
3. Public Wi-Fi Berlin. URL `http://www.visitberlin.de/en/article/w-lan-for-all-public-wi-fi-berlin`

4. Wireless@SG. URL http://www.ida.gov.sg/Learning/Technology-You/Wireless-SG
5. Balasubramanian, N., Balasubramanian, A., Venkataramani, A.: Energy consumption in mobile phones: a measurement study and implications for network applications. In: Proceedings of the ACM SIGCOMM conference on Internet measurement, pp. 280–293. ACM, New York, NY, USA (2009)
6. Burger, V., Seufert, M., Kaup, F., Wichtlhuber, M., Hausheer, D., Tran-Gia, P.: Impact of WiFi Offloading on Video Streaming QoE in Urban Environments. In: IEEE Workshop on Quality of Experience-based Management for Future Internet Applications and Services (QoE-FI). London, UK (2015)
7. Chen, S., Yuan, Z., Muntean, G.M.: An Energy-aware Multipath-TCP-based Content Delivery Scheme in Heterogeneous Wireless Networks. In: Proceedings of the IEEE Wireless Communications and Networking Conference (WCNC). Shanghai, China (2013)
8. Cisco: Cisco Visual Networking Index: Global Mobile Data Traffic Forecast Update, 2014-2019. Tech. rep., Cisco (2015)
9. Dimatteo, S., Hui, P., Han, B., Li, V.O.: Cellular Traffic Offloading Through WiFi Networks. In: 8th IEEE International Conference on Mobile Adhoc and Sensor Systems (MASS). Valencia, Spain (2011)
10. Donelson, L.J., Sweet, C.W.: Method, Apparatus and System for Wireless Network Authentication Through Social Networking (2012). US Patent App. 13/287,931
11. Gladisch, A., Daher, R., Tavangarian, D.: Survey on Mobility and Multihoming in Future Internet. Wireless Personal Communications **74**(1) (2014)
12. Gonzalez, M., Higashino, T., Okada, M.: Radio Access Considerations for Data Offloading with Multipath TCP in Cellular/WiFi Networks. In: Proceedings of the International Conference on Information Networking (ICOIN). Bangkok, Thailand (2013)
13. Huang, J., Quian, F., Gerber, A., Mao, Z.M., Sen, S., Spatscheck, O., Qian, F.: A Close Examination of Performance and Power Characteristics of 4G LTE Networks. In: MobiSys, pp. 225–238 (2012)
14. Kaup, F., Jomrich, F., Hausheer, D.: Demonstration of NetworkCoverage – A Mobile Network Performance Measurement App. In: Proceedings of the International Conference on Networked Systems (NetSys 2015). Cottbus, Germany (2015)
15. Kaup, F., Wichtlhuber, M., Rado, S., Hausheer, D.: Can Multipath TCP Save Energy? A Measuring and Modeling Study of MPTCP Energy Consumption. In: IEEE LCN (2015)
16. Khadraoui, Y., Lagrange, X., Gravey, A.: A Survey of Available Features for Mobile Traffic Offload. In: Proceedings of the 20th European Wireless Conference. Barcelona, Spain (2014)
17. Lafuente, C.B., Titi, X., Seigneur, J.M.: Flexible Communication: A Secure and Trust-Based Free Wi-Fi Password Sharing Service. In: Proceedings of the 10th IEEE International Conference on Trust, Security and Privacy in Computing and Communications (TrustCom). Changsha, China (2011)
18. Mamatas, L., Psaras, I., Pavlou, G.: Incentives and Algorithms for Broadband Access Sharing. In: Proceedings of the ACM SIGCOMM Workshop on Home Networks. New Delhi, India (2010)
19. Paasch, C., Detal, G., Duchene, F., Raiciu, C., Bonaventure, O.: Exploring Mobile/WiFi Handover with Multipath TCP. In: Proceedings of the ACM SIGCOMM Workshop on Cellular Networks: Operations, Challenges, and Future Design. Helsinki, Finland (2012)

20. Panitzek, K., Schweizer, I., Bönning, T., Seipel, G., Mühlhäuser, M.: First Responder Communication in Urban Environments. International Journal of Mobile Network Design and Innovation **4**(2), 109–118 (2012)
21. Ramos-Muñoz, J.J., Prados-Garzon, J., Ameigeiras, P., Navarro-Ortiz, J., López-Soler, J.M.: Characteristics of Mobile YouTube Traffic. IEEE Wireless Communications **21**(1), 18–25 (2014)
22. Rosen, S., Yao, H., Nikravesh, A., Jia, Y., Choffnes, D., Mao, Z.M.: Demo: Mapping Global Mobile Performance Trends with Mobilyzer and MobiPerf. In: Proceedings of the 12th International Conference on Mobile Systems, Applications, and Services (MobiSys 2014). Bretton Woods, NH, USA (2014)
23. Rossi, C., Vallina-Rodriguez, N., Erramilli, V., Grunenberger, Y., Gyarmati, L., Laoutaris, N., Stanojevic, R., Papagiannaki, K., Rodriguez, P.: 3GOL: Power-boosting ADSL using 3G OnLoading. In: Proceedings of the 9th Conference on Emerging Networking Experiments and Technologies (CoNEXT). Santa Barbara, CA, USA (2013)
24. Sastry, N., Crowcroft, J., Sollins, K.: Architecting Citywide Ubiquitous Wi-Fi Access. In: Proceedings of the 6th Workshop on Hot Topics in Networks (HotNets). Atlanta, GA, USA (2007)
25. Seufert, M., Burger, V., Hoßfeld, T.: HORST - Home Router Sharing based on Trust. In: Proceedings of the Workshop on Social-aware Economic Traffic Management for Overlay and Cloud Applications (SETM 2013). Zurich, Switzerland (2013)
26. Singh, S., Dhillon, H.S., Andrews, J.G.: Offloading in Heterogeneous Networks: Modeling, Analysis, and Design Insights. IEEE Transactions on Wireless Communications **12**(5), 2484–2497 (2013)
27. Sonntag, S., Manner, J., Schulte, L.: Netradar-Measuring the wireless world. In: Proceedings of the 11th International Symposium on Modeling & Optimization in Mobile, Ad Hoc & Wireless Networks (WiOpt 2013). Tsukuba Science City, Japan (2013)
28. Vidales, P., Manecke, A., Solarski, M.: Metropolitan Public WiFi Access Based on Broadband Sharing. In: Proceedings of the Mexican International Conference on Computer Science (ENC 2009). Mexico City, Mexico (2009)
29. Wireless Broadband Alliance: WBA Industry Report 2011: Global Developments in Public Wi-Fi. Tech. rep. (2011)
30. Wittie, M.P., Stone-Gross, B., Almeroth, K.C., Belding, E.M.: MIST: Cellular Data Network Measurement for Mobile Applications. In: Proceedings of the 4th International Conference on Broadband Communications, Networks and Systems (BROADNETS 2007). Raleigh, NC, USA (2007)
31. Zhang, L., Tiwana, B., Dick, R.P., Qian, Z., Mao, Z., Wang, Z., Yang, L.: Accurate Online Power Estimation and Automatic Battery Behavior Based Power Model Generation for Smartphones. In: CODES + ISSS'10. ACM (2010)